Latin American Journal of Aquatic Research, 54(1): 15-28, 2026
DOI: 10.3856/vol54-issue1-fulltext-3363

Research Article

Spatial and temporal variability of sea surface temperature anomalies in the Eastern Pacific Ocean (2000-2020): implications for ENSO monitoring

Aura Buenfil-Ávila[1], Sofia Ortega-García[1], Ulianov Jakes-Cota[1]
Rodrigo Moncayo-Estrada[1], Gabriel Reygondeau[2] & Héctor Villalobos[1]
[1]Instituto Politécnico Nacional, Centro Interdisciplinario de Ciencias Marinas (CICIMAR-IPN), La Paz BCS, México
[2]Changing Ocean Research Unit, Institute for the Oceans and Fisheries University of British Columbia, Vancouver, Canada
Corresponding author: Héctor Villalobos (hvillalo@ipn.mx)

ABSTRACT. Sea temperature anomaly events play a fundamental role in the environmental variability within the Eastern Pacific Ocean (EPO). However, the magnitude and spatial extent of these events should be acknowledged, as they are not uniform across all areas. A comprehensive understanding of this variability is necessary for regional analyses. The present study used sea surface temperatures (SST; 2000-2020) from the Global Ocean Ensemble Physics Reanalysis database to represent the spatial distribution of SST anomalies within the EPO during four intense El Niño Southern Oscillation (ENSO) events. Additionally, time series of anomalies based on the Extended Reconstructed Sea Surface Temperatures database were obtained for uniformly selected quadrants along the EPO, as well as for its main currents and water masses. The findings revealed significant differences between prominent ENSO events and certain EPO areas: the central EPO showed a higher frequency, whereas others, such as the Costa Rica Dome, showed a lower frequency, particularly during La Niña events. Furthermore, the present study identified disparities when comparing the outcomes reported by the main El Niño regions widely used for ENSO identification. For instance, while La Niña 2000/01 and El Niño 2002/03 were identified by the Oceanic El Niño Index and the El Niño 3 and El Niño 4 indices, these events were not observed in all the EPO. Likewise, certain events showing clear warm-anomaly trends, such as those in 2017/18, were classified by the indices as cold periods. In contrast, strong events such as La Niña 2010/11 and El Niño 2014/16 were consistently identified in all selected areas in the EPO, in coincidence with the indices.

Keywords: SST anomaly; climatology; ERSST; ENSO; climate variability; ONI

INTRODUCTION

The climatic and oceanic conditions in the Eastern Pacific Ocean (EPO) and their variability are influenced by a range of interdependent factors, including ocean currents, trade winds, upwelling, and anomalous warming or cooling events. Among these, the El Niño-Southern Oscillation (ENSO) is a key driver of climatic variability in the region. ENSO events are recurrent fluctuations in sea surface temperatures (SST) and atmospheric pressure that show a periodicity from two to six years, exhibiting two phases: a warm El Niño and a cold La Niña (An & Wang 2000). During El Niño, weak trade winds favor warm-water flux from west to east, while rainfall moves eastward, causing flooding along the coasts of

Associate Editor: Marcela Cornejo

South America. During La Niña, trade winds strengthen, and more rainfall occurs over the western tropical Pacific; winds near the equator drive westward warm water and bring eastward cold surface water (Fedorov & Philander 2000). ENSO nature is complex. The various positive and negative feedback processes in ocean-atmosphere interactions are responsible for the diversity of ENSO events in their regional patterns, magnitudes, and temporal evolution (Timmermann et al. 2018). El Niño events that exhibit a greater degree of warming in the Eastern Pacific are referred to as El Niño EP or canonical El Niño, whilst those that occur in the Central Pacific and warm pool region are referred to as El Niño CP or El Niño Modoki (Ashok et al. 2007). El Niño EP typically ends later in the boreal spring than El Niño CP because of the collapse of the trade winds, which suppresses the thermocline's depth (Lengaigne & Vecchi 2010). A coastal El Niño is also recognized, with SST anomalies present in the Eastern Pacific off the coast of South America (Takahashi & Martínez 2019). On the other hand, the spatial patterns of La Niña occurrences are less diverse, mainly because they are weaker (Kug & Ham 2011).

The diversity of ENSO events has led to the construction of different indices to determine their occurrence. To name a few, the Multivariate ENSO Index (MEI) considers anomalies of sea level pressure, SST, surface zonal and meridional winds, and outgoing long-wave radiation. The Southern Oscillation Index (SOI) is built on the comparison of sea level pressure between Tahiti and Darwin, Australia. The Oceanic El Niño Index (ONI) measures whether a warm or cold phase is present based on SST anomalies: El Niño (≥ 0.5°C) and La Niña (≤ -0.5°C), further classified as weak ((|0.5-1.0|°C) or strong (|1.5-2.0|°C). The ONI is based on the analysis of the Extended Reconstructed Sea Surface Temperature (ERSST) database (Huang et al. 2017). Three-month moving averages of SST anomalies are calculated for the so-called El Niño 3.4 region (5°S-5°N; 170-120°W). Other regions used to construct SST anomaly-based indices include El Niño 1+2 (0-10°S; 90-80°W), El Niño 3 (5°S-5°N; 150-90°W), and El Niño 4 (5°S-5°N; 170°E-150°W). In all cases, anomalies are calculated using 30-year baselines updated every five years to remove the warming trend. For instance, 2000-2005 anomalies are calculated with the average year from 1985-2015, while the 2005-2010 anomalies use a 1990-2020 baseline.

Due to its simplicity, the ONI is one of the most widely used indices. It has been employed as a variability indicator in modelling the habitat preferences of marine species, often implicitly assuming that the spatial distribution of ENSO events is homogeneous and synchronous across the EPO (Farchadi et al. 2019, Díaz-Delgado et al. 2021, Feng et al. 2022, Félix-Salazar et al. 2024). Given the high diversity of ENSO events, incorporating the ONI or any other index as an explanatory variable to characterize ENSO impacts on marine species could be biased, potentially affecting the interpretations of these phenomena. In this context, we present an analysis of SST anomalies in the EPO from 2000 to 2020 to identify differences in the timing and spatial extent of ENSO events in this region. The objectives were 1) to characterize the spatial evolution of the main events identified; 2) to compare the variation of the anomalies in typical locations of the main currents and water masses of the EPO; and 3) to contrast the main SST anomaly-based ENSO indices with the EPO regional anomaly analysis.

MATERIALS AND METHODS

Two sources of data with different spatial resolutions were considered in the present study, (1) sea water potential temperature (0.25°×0.25°), included in the Global Ocean Ensemble Physics Reanalysis product (doi: 10.48670/moi-00024) from the Copernicus Marine Service of the European Space Agency, was used to calculate spatial anomalies in the EPO; and (2) the coarser (2°×2°) ERSST dataset was used to characterize the temporal variability of the anomalies associated to selected ocean currents and water masses in the region.

Spatial sea surface temperature anomalies

Four intense ENSO events (La Niña 2007/08 and 2010/11; El Niño 2009/10 and 2014/16) were chosen by inspecting the values of the ONI (https://origin.cpc.ncep.noaa.gov/products/analysis_monitoring/ensostuff/ONI_v5.php) in accordance with the 0.5°C threshold. The start and end months of each event were taken as the middle of the three-month moving averages as shown (Table 1). A graphical representation of the ONI with these four events marked with rectangles is included at the top of Figure 4. The SST anomalies at the quadrant (0.25°×0.25°) level during these events were calculated with functions from the satin package (Villalobos & González-Rodríguez 2022) for the R programming language environment (R Core Team 2023). For this purpose, monthly data from the Copernicus product mentioned above were used. This dataset was built with a numerical ocean model (NEMO) on the ORCA025 grid, with satellite data assimilation and in situ data from the CORA database

Table 1. Comparison of observed frequencies (O) of the number of Extended Reconstructed Sea Surface Temperatures (ERSST) quadrants, and the standardized Pearson residual (χ_p) per year with a given condition (Neg: negative; Neu: neutral; and Pos: positive anomalies) in the Eastern Pacific Ocean (EPO) and the El Niño Southern Oscillation (ENSO) events, according to the Oceanic Niño Index (ONI). The period refers to the duration of each event. ENSO events highlighted in blue (La Niña) and red (El Niño) are shown in Figure 2. The total number of quadrants per year is the sum of 80 quadrants per month (i.e. 80 × 12).

Year	O			χ_p			ENSO events according to ONI	Period
	Neg	**Neu**	**Pos**	**Neg**	**Neu**	**Pos**		
2000	113	796	51	4.7	11.3	-16.1	La Niña	2000/01-2001/02
2001	62	759	139	-1.3	9.7	-11.4		
2002	32	606	322	-4.8	3.1	-1.6	El Niño	2002/06-2003/02
2003	13	590	357	-7.0	2.4	0.2		
2004	9	602	349	-7.5	2.9	-0.2	El Niño	2004/07-2005/02
2005	56	650	254	-2.0	5.0	-5.2	La Niña	2005/11-2006/03
2006	22	569	369	-6.0	1.5	0.9	El Niño	2006/09-2007/01
2007	199	628	133	14.8	4.0	-11.7	La Niña	2007/06-2008/06
2008	144	663	153	8.3	5.6	-10.6	La Niña	2008/11-2009/03
2009	35	372	553	-4.4	-7.0	10.7	El Niño	2009/07-2010/03
2010	241	544	175	19.7	0.4	-9.5	La Niña	2010/06-2011/05
2011	257	663	40	21.6	5.6	-16.6	La Niña	2011/07-2012/04
2012	76	541	343	0.4	0.3	-0.5		
2013	54	820	86	-2.2	12.3	-14.2		
2014	14	388	558	-6.9	-6.3	10.9	El Niño	2014/10-2016/04
2015	1	189	770	-8.4	-14.9	22.2		
2016	2	217	741	-8.3	-13.7	20.7	La Niña	2016/08-2016/12
2017	43	347	570	-3.5	-8.1	11.6	La Niña	2017/11-2018/04
2018	53	424	483	-2.3	-4.8	6.9	El Niño	2018/09-2019/06
2019	4	367	589	-8.1	-7.2	12.6		
2020	99	492	369	3.1	-1.8	0.9	La Niña	2020/08-2020/12

(Lellouche et al. 2013). Monthly anomalies (a_{xyij}) were calculated per quadrant by subtracting the corresponding average year (baseline from 1993 to 2020) according to:

$$a_{xyij} = z_{xyij} - \bar{z}_{xyj},$$

where z_{xyij} is the potential temperature at the surface for the quadrant with longitude x, latitude y, in the year i and month j, and $\bar{z}_{xyj} = \frac{\sum_{i=1}^{n} z_{xyij}}{n}$ is the average for the month j in the quadrant (x, y) over the n = 28 years considered as baseline.

To graphically visualize the events' spatial development over time, the monthly anomalies were mapped for four selected months from each event: one at the beginning, two at the peak, and one at the end.

Interannual variability in the sea surface temperature anomalies

Eighty ERSST quadrants distributed uniformly in the EPO were selected (Fig. 1); the ERSST dataset is a monthly global analysis derived from the International Comprehensive Ocean-Atmosphere Dataset (ICOADS). The anomalies per quadrant were calculated as previously described and subsequently smoothed using a 3-month moving average (k = 3), consistent with the ONI definition. For this purpose, the smooth R package (Svetunkov 2023) was used to obtain centered moving averages by first computing the simple moving average as a state-space model with backcasting. This iterative initialization mechanism preserves the initial k data points (Svetunkov & Petropoulos 2017), and then shifts the series back in time (Svetunkov 2017). Afterwards, to characterize the anomaly pattern during the selected period, the frequencies of quadrants with negative (≤ -0.5°C), neutral (-0.5 to 0.5°C), and positive (≥ 0.5°C) anomalies were obtained by year. These observed frequencies (O) were analyzed as a contingency table to evaluate independence between variables and to identify where the differences between observed and expected frequencies are greatest (Legendre & Legendre 1998). For this purpose, the expected fre-

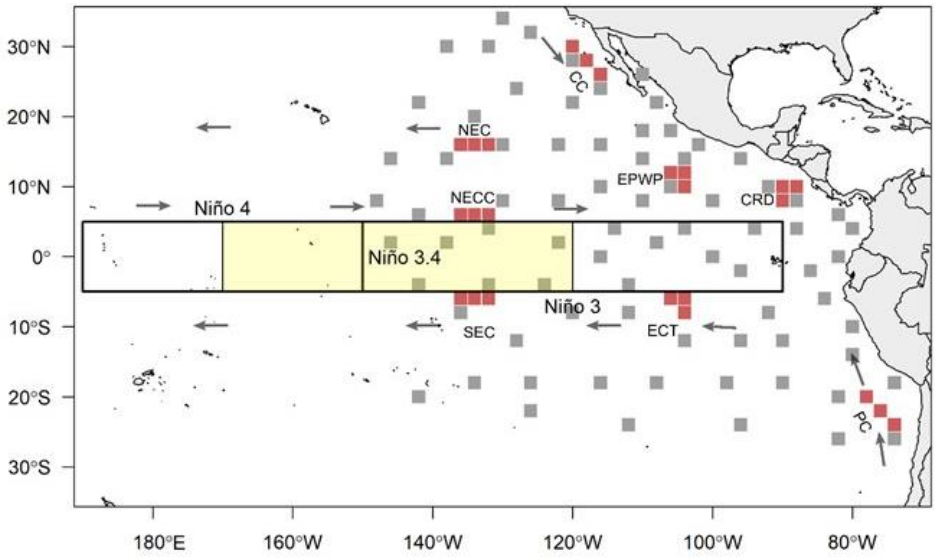

Figure 1. Eastern Pacific Ocean (EPO, from 150°W to the American coastline) showing the Extended Reconstructed Sea Surface Temperatures (ERSST) quadrants (2°×2°) selected for the analysis. Gray squares were used to quantify the proportion of negative (≤ -0.5°C), neutral (-0.5 to 0.5°C), and positive (≥ 0.5°C) quadrants per year. Red squares were considered representative of the main hydrographic features in the EPO and were used to analyze temporal variability in anomalies. The location of currents and water masses was taken from Fiedler & Talley (2006). CC: California Current; NEC: North Equatorial Current; NECC: North Equatorial Countercurrent; SEC: South Equatorial Current; EPWP: Eastern Pacific Warm Pool; CRD: Costa Rica Dome; ECT: Equatorial Cold Tongue; and PC: Peru Current. El Niño regions that were used to compare with the regional SST anomalies are also shown: El Niño 4 region, El Niño 3.4 region (yellow rectangle), and El Niño 3 region.

quencies (E) were calculated under the hypothesis of independence between the year and the prevailing anomaly conditions (i.e. negative, neutral, or positive) by multiplying the marginal totals of O, and dividing by the total number of observations, according to:

$$E = \frac{r_i c_j^T}{\sum_{i=1}^{m}\sum_{j=1}^{n} O_{ij}},$$

where $r_i = \sum_{j=1}^{n} O_{ij}$ are the sums of the i-th row (years), and $c_j = \sum_{i=1}^{m} O_{ij}$ are the sums of the j-th column (condition).

To test the differences between expected and observed frequencies, the standardized Pearson residuals (χ_p) were computed:

$$\chi_p = \frac{(O-E)}{\sqrt{E}},$$

which were contrasted with the critical value:

$$\chi_p^2\ crit. = \sqrt{\chi_{\alpha,\upsilon}^2 / n.entries},$$

where $\chi_{\alpha,\upsilon}^2$ is the chi-squared probability for $\sum_{i=1}^{m}\sum_{j=1}^{n}(O_{ij} - E_{ij})^2 / E_{ij}$ with υ = (*n. rows*-1)(*n. cols*. -1) degrees of freedom.

For every combination of year and anomaly condition, significant differences were present when the corresponding $\chi_p > \chi_p^2\ crit.$ The observed frequencies were represented in a stacked barplot, and a comparative table between O and χ_p was constructed, highlighting combinations where $\chi_p > 4$, indicating a larger-than-expected number of quadrants in a given category (negative, neutral, or positive anomalies).

In addition, three ERSST quadrants were selected from the typical locations schematized by Fiedler & Talley (2006) of each of the eight major currents and water masses in the EPO. Each set of three quadrants was averaged and hereafter will be considered as proxies of the California Current (CC); North Equatorial Current (NEC); North Equatorial Countercurrent (NECC); South Equatorial Current (SEC); Eastern Pacific Warm Pool (EPWP); Costa Rica Dome (CRD); Equatorial Cold Tongue (ECT); and Peru Current (PC) (Fig. 1). The time series anomalies for each one of the hydrographic features were calculated and smoothed with centered moving averages and compared with the indices for the main El Niño regions (3, 3.4, and 4) to find similarities and differences in the identification of

SST anomaly events across the EPO. Finally, a correlation analysis was also done to complement the comparison.

RESULTS

Spatial sea surface temperature anomalies

The SST anomaly distribution maps show that ENSO events vary in duration, intensity, and spatial extent (Fig. 2). La Niña 2007/08 had a reduced spatial extent and lower intensity than La Niña 2010/11, which reached SST anomalies of ~-4°C. In both events, the main sites showing the highest negative anomaly values were near the CC, SEC, ECT, and PC. The 2009/10 and 2014/16 El Niño events also showed differences in extent and duration (~9 months *vs.* 1.5 years, respectively). While the former had a maximum anomaly of 2°C, the latter had a stronger intensity, hovering around 4°C. Below is a more detailed description of each event.

La Niña 2007/08

At the beginning of La Niña in June 2007, negative anomalies were observed in CC, SEC, ECT, and PC. In December 2007-January 2008, during the peak of this cold event, the negative SST anomalies extended to all EPO areas, with the lowest values (~-3°C) observed within the Gulf of California and near CC, CRD, ECT, and SEC. Finally, negative anomalies were observed mostly between 130-115°W and 20-35°N at the end of this phase, in June 2008. Positive anomalies (~2°C) were observed in some areas at the end of the event, including the vicinity of the Galapagos Islands and latitudes between 10-30°S.

El Niño 2009/10

El Niño 2009/10 was a brief event that started in July 2009, with anomalies spreading across the EPO, with the highest values around the Galapagos Islands, ECT, and SEC. Positive 2°C anomalies expanded to the American coast and the CRD and EPWP during the highest anomaly peak (December 2009-January 2010); CC and PC were the least affected by these conditions. This process ended in March 2010, with a reduction in positive anomaly distribution, which was mostly concentrated along the equator in SEC and ECT.

La Niña 2010/11

This event was more intense than the previous cold event, with negative anomalies spanning a larger area. This event began in June 2010 with negative anomalies (~-2°C) near CC, ECT, SEC, and PC, where the least vulnerable sites to negative anomalies were CRD and between 10-30°S and 150-120°W. Negative anomalies covered the EPO and extended into the CRD and EPWP during the peak in November-December 2010, reaching ~-4°C in locations around ECT and SEC. Positive anomalies began to occur in the middle of the EPO (from 10°S to 20°N) during the last phase of this event (May 2011). In contrast, regions with negative anomalies that persisted were near CC and PC, and at latitudes 10-20°S.

El Niño 2014/16

El Niño 2014/16 was the longest-lasting (1.5 years) and most dramatic of the events in the last 20 years. The first phase began in October 2014, with an expansion of positive anomalies across a large portion of the EPO, which coincided with the Warm Blob (Di Lorenzo & Mantua 2016) that extended along the Baja California Peninsula, reaching the highest positive anomalies (4°C); negative anomalies were also detected at latitudes ranging from 10 to 25°S. October-November 2015 were the most well-represented peak months, showing anomalies of 2°C extending throughout most of the EPO, with the greatest anomaly values (4°C) around the equator and off the coast of Baja California, where the Warm Blob was observed. The last phase of this event in April 2016 still exhibited a preponderance of positive anomalies; however, several places displayed negative anomalies, including the coasts of Colombia and Ecuador, as well as the Galapagos Islands.

Interannual variability in sea surface temperature anomalies

According to the frequencies of ERSST quadrants with different conditions by year, a higher proportion (>0.5) of neutral anomalies was observed for most of the analyzed years, especially between 2000 and 2008, 2010 to 2013, and 2020 (Fig. 3). During 2009, and from 2014 to 2019, the number of quadrants with positive anomalies prevailed. On the contrary, a predominance of quadrants with negative anomalies was not observed during the analyzed period, attaining maximum proportions of approximately 20% only in 2007, 2010, and 2011.

The analysis of standardized Pearson residuals for differences between the observed and expected numbers of quadrants in each condition revealed large discrepancies relative to the ONI (Table 1). During La Niña conditions in 2000, there was a higher than expected (χ_p = 11.3) number of quadrants with neutral conditions.

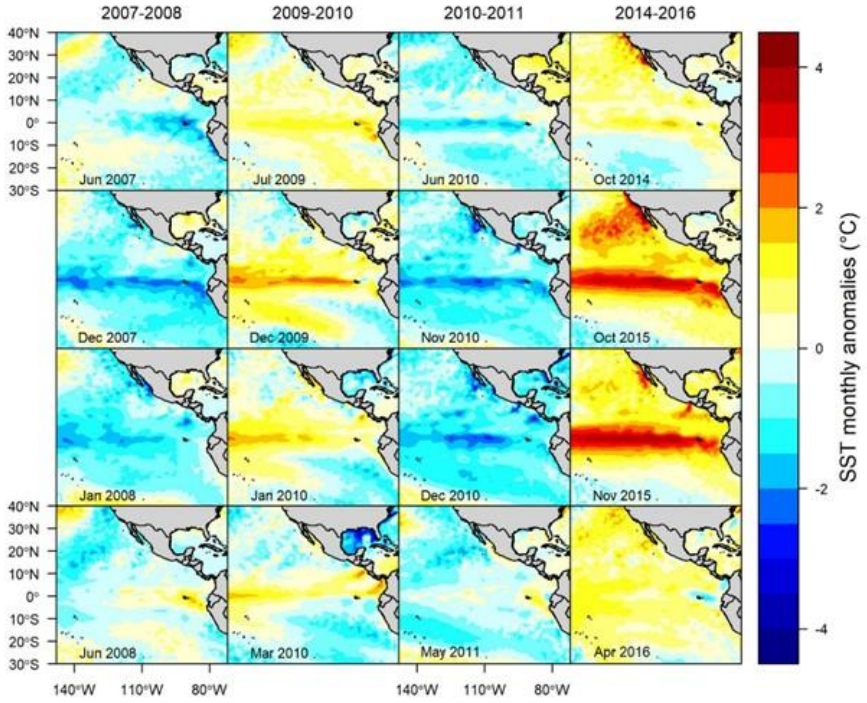

Figure 2. Maps of sea surface temperatures (SST) anomalies summarizing the development of four ENSO events. From left to right, La Niña 2007/08; El Niño 2009/10; La Niña 2010/11; and El Niño 2014/16. For every ENSO event, the upper row represents the beginning, the two middle rows the peak, and the lower row the end.

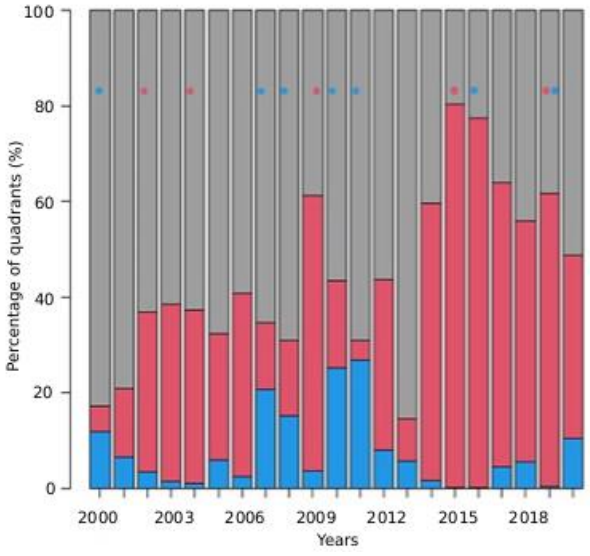

Figure 3. Quadrant percentage with negative (< -0.5°C; blue), neutral (-0.5 to 0.5°C; gray), and positive (> 0.5°C; red) anomalies by year from 2000 to 2020. The blue and red circles represent El Niño Southern Oscillation (ENSO) events according to the Oceanic El Niño Index (ONI) (i.e. when three consecutive periods exceeded the 0.5°C threshold).

Other weak events not reflected in the residuals were El Niño 2002/03, El Niño 2004/05, La Niña 2005/06, El Niño 2006/07, La Niña 2016, La Niña 2017/18, and La Niña 2020. On the contrary, the high Pearson residuals for the number of quadrants with negative anomalies during 2007, 2008, 2010, and 2011 (14.8, 8.3, 19.7, 21.6, respectively) agreed with La Niña conditions observed in the ONI during those years. Similarly, El Niño 2009/10, 2014/16, and 2018/19 were matched with Pearson residuals for the higher-than-expected number of quadrants with positive anomalies in the corresponding years.

The comparison of SST time-series anomalies representing the main hydrographic features in the EPO with the ONI and indices for the El Niño 3 and El Niño 4 regions is shown (Fig. 4). In general terms, the indices show agreement, with the ONI and El Niño 3 showing the highest correlation (0.94), followed closely by the ONI and El Niño 4 (0.91). In contrast, the correlation between El Niño 3 and El Niño 4 was 0.77 (Fig. 5). La Niña conditions in 2000/01 were observed only in the first months of 2000 in the NECC and the CRD, and in the second half of that year in the CC. Similarly, El Niño 2002/03 was only mirrored in the NECC, the SEC, and the CRD, but with a lag. La Niña conditions at the end of 2005 and the beginning of 2006 were

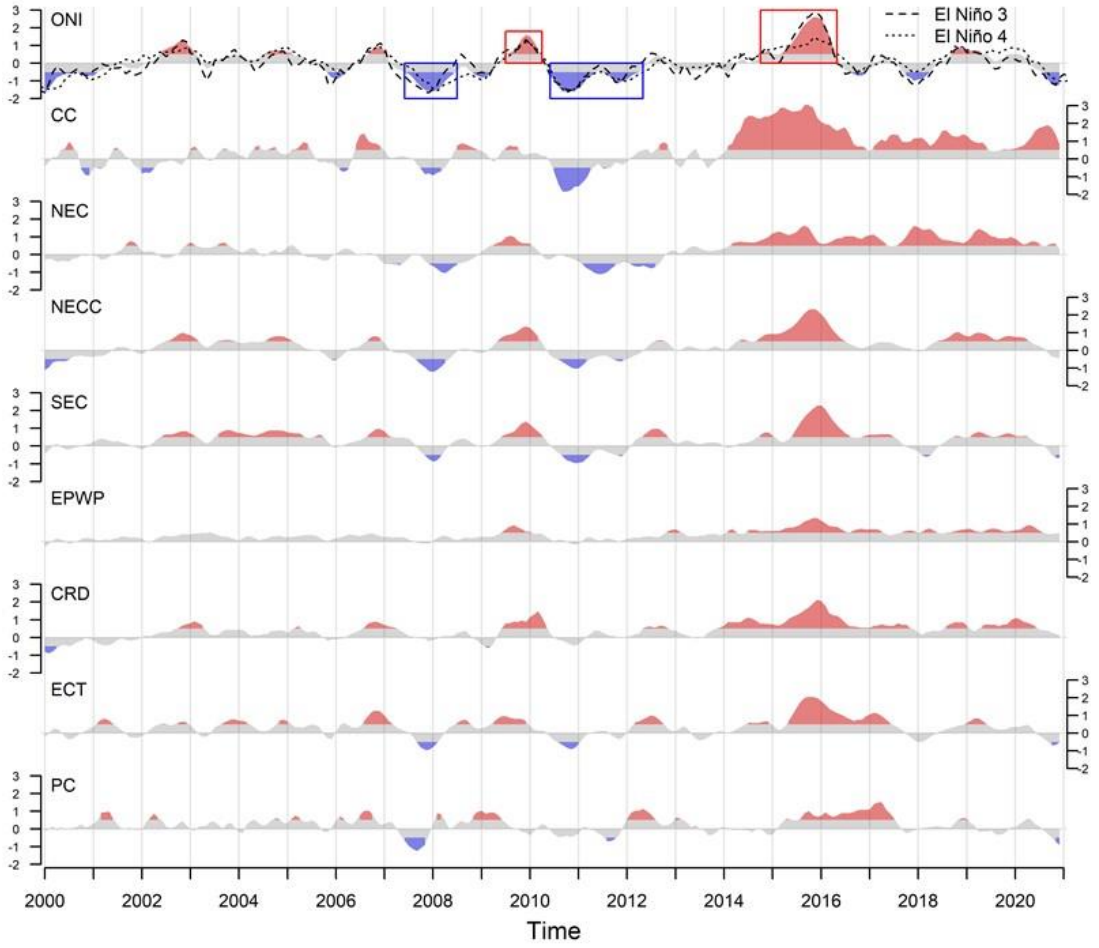

Figure 4. Time series (2000-2020) of the Oceanic El Niño Index (ONI), El Niño 3, El Niño 4, and the anomalies of the currents and water masses in the Eastern Pacific Ocean (EPO). Rectangles in blue (La Niña) and red (El Niño) denote the ENSO events shown in Figure 2. Negative anomalies (≤ -0.5°C) are shown in blue; positive (≥ 0.5°C) anomalies in red. CC: California Current; NEC: North Equatorial Current; NECC: North Equatorial Countercurrent; SEC: South Equatorial Current; EPWP: Eastern Pacific Warm Pool; CRD: Costa Rica Dome; ECT: Equatorial Cold Tongue; and PC: Peru Current.

marginally detected in the CC and the NECC, but nowhere else. On the contrary, the warm and cold events from 2006 to 2011 appear to be more extended in the EPO. Likewise, the strong El Niño 2015/16 was identified in all selected currents and water masses, with varying durations. Finally, the cold conditions between the end of 2016 and 2018, and in 2020, were barely observed, occurring only in the SEC, the ECT, and the PC. It is interesting to note that, since 2014, warm conditions have prevailed across all selected areas.

Considering a cut-off value of 0.7, the NECC, SEC, and CRD showed high correlations with the ONI (0.95, 0.89, and 0.77, respectively), El Niño 3 (0.86, 0.85, and 0.73, respectively), and El Niño 4 (0.9, 0.78, and 0.77, respectively). The ECT was correlated only with El Niño 3 (0.85) and the ONI (0.76). The remaining features (CC, NEC, EPWP, and PC) had correlations <0.64 with the three indices. The PC showed the lowest correlations with the indices (0.17-0.38) and with the other features, reflected in the scatter plots, which did not show a trend, unlike the NECC, which showed clear linear relationships with the indices (Fig. 5).

DISCUSSION

The present study identified variations in spatial extent and intensity among ENSO events. This climate pattern, characterized by its recurrence, often exhibits inconsistent characteristics that challenge generalization. Factors as strength, initial and maturing phases, duration, and spatial coverage may vary from event to

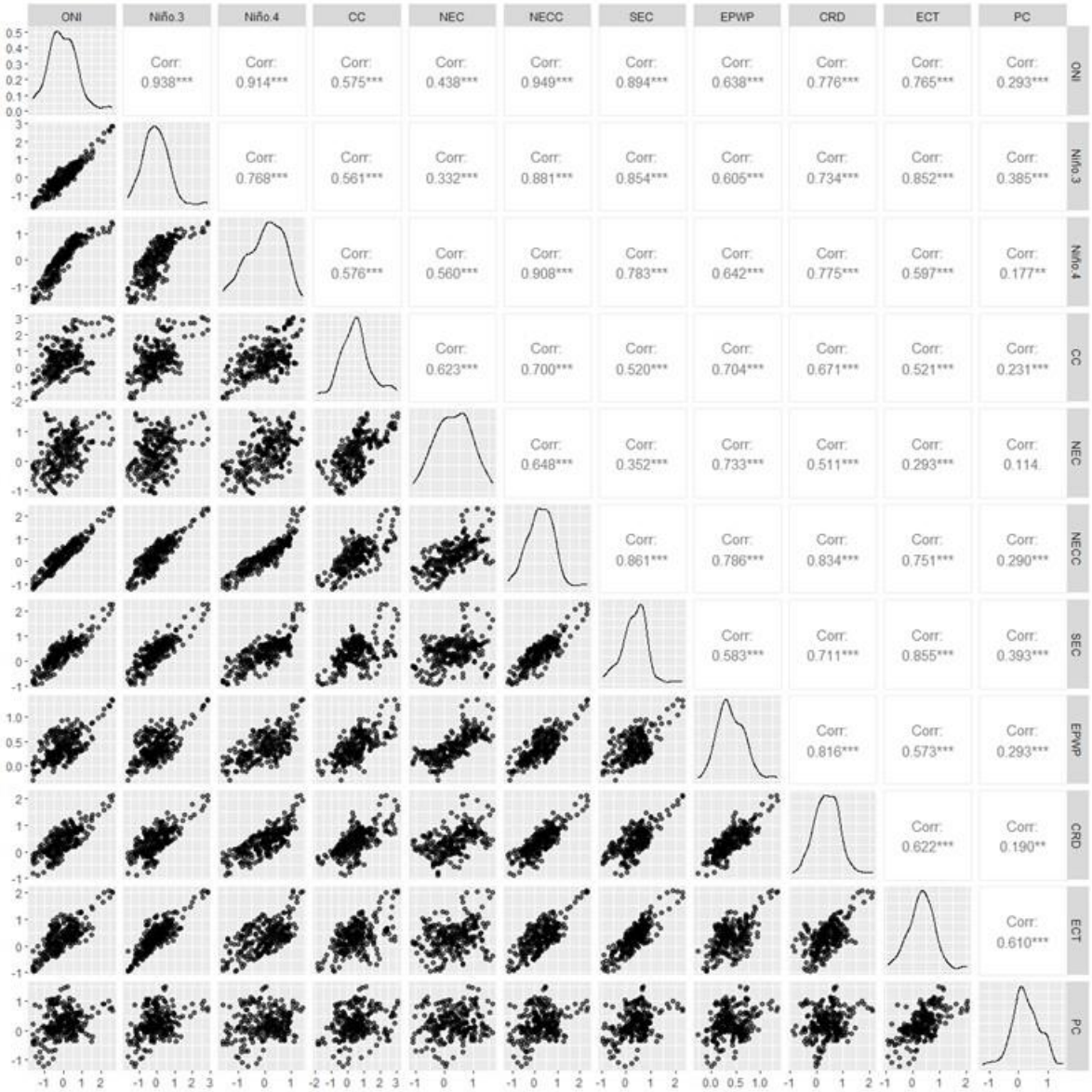

Figure 5. Pearson correlation coefficients and scatter plots between the anomalies of the currents and water masses in the Eastern Pacific Ocean (EPO) and the Niño regions. CC: California Current; NEC: North Equatorial Current; NECC: North Equatorial Countercurrent; SEC: South Equatorial Current; EPWP: Eastern Pacific Warm Pool; CRD: Costa Rica Dome; ECT: Equatorial Cold Tongue; and PC: Peru Current. Asterisks indicate statistical significance ($\alpha = 0.05$).

event (Horii & Hanawa 2004); consequently, ENSO event impacts are not consistent across all EPO regions. The most intense event observed in the EPO within the analyzed time series was the El Niño 2014/16, whose effects have been well documented. These include changes in wind patterns that led to decreases in phytoplankton biomass in the Eastern North Pacific (Whitney 2015) and impacts on regional fisheries such as the market squid (*Doryteuthis opalescens*) in California (NMFS 2017, Lehodey et al. 2021). This event also coincided with the Warm Blob (Di Lorenzo & Mantua 2016), which extended from the Northeastern Pacific southward to approximately 18-20°N (Ramos-Rodríguez et al. 2020). This patch of warm water was concentrated mainly in the CC and intensified toward the end of 2014, peaking in fall 2015. This phenomenon caused multiple impacts on marine life in the region, including toxic algal blooms (McCabe et al. 2016) and seabird mortality (Gibble et al. 2018).

Understanding regional SST spatial variability is highly relevant for identifying the regions most susceptible to anomalous events. Furthermore, ENSO events can affect the circulation patterns of the main EPO currents, especially those that are strongly linked and serve as transport channels for ENSO oscillations, such as NEC, SEC, and NECC. In the same way, the changes that may occur in these current systems will depend on the type of event (i.e. El Niño EP or El Niño CP). For example, during El Niño EP, the equatorial winds weaken, which is directly reflected in the SEC, which also weakens. During the development of strong El Niño EP events, the NECC intensifies and shifts southward due to changes in wind stress driven by Rossby waves (Chen et al. 2016), whereas in El Niño CP, the NECC is weaker (Tan & Zhou 2018). During El Niño, the NEC bifurcation shifts northward, increasing the flow of neighboring currents (Hu et al. 2015). In the present analysis, however, no attempts have been made to classify the El Niño events as either EP or CP.

During La Niña, the Peru and California currents show more pronounced negative anomalies, confirming that these two current systems are the least susceptible to sea warming, attributed to increased upwelling due to global warming (Belkin 2009), which causes changes in land-ocean air circulation patterns, enhancing winds that favor upwelling and decrease the SST (Bakun 1990). During El Niño 2009/10 and 2014/16, positive anomalies were observed in all sampled areas, albeit with lower intensity in the PC, showing that coastal zones near these massive current systems may be affected by El Niño events, mainly because equatorward Kelvin waves are trapped there, leading to an accumulation of energy (Sprintall et al. 2020). Also, during La Niña, the EPWP and the CRD exhibited lower susceptibility, which may be due to the EPWP's spatial extent variability but not its SST range, with local heat fluxes and oceanic advection as the primary drivers of these conditions (Wang & Fiedler 2006). The CRD, on the other hand, does not exhibit high SST variability due to key factors that help maintain its conditions, namely the presence of the Papagayo jet from the north during winter and trade wind convergence in the Intertropical Convergence Zone during summer (Kessler 2006).

Among the various regions used for monitoring ENSO events, the El Niño 3 region was previously the most widely used. However, it was later determined that the El Niño 3.4 region (used for the ONI) constitutes a more strategic monitoring area for both El Niño EP and El Niño CP, while El Niño 4 region is supposed to present less variance in identifying ENSO events (Trenberth & Stepaniak 2001); in addition, due to their proximity, El Niño 4 region is more suitable for identifying CP events. The El Niño 1+2 region, located near the coasts of South America, is mainly used to detect local events and is highly variable (Trenberth & Hoar 1996). Consequently, defining ENSO phases in this region is challenging, as it typically responds less to broader warming and cooling and can even yield false positives (Hanley et al. 2003). This index showed high correlations only with El Niño 3 (0.79) and the ECT (0.77); therefore, it was excluded from the analysis.

It is important to mention that imbalances can occur in both atmospheric and oceanic components between ENSO events (Hanley et al. 2003). An instance of such imbalances occurred during El Niño 2004/05, which was situated in the West-Central Pacific, encompassing the El Niño 3 and El Niño 4 regions. Despite SST anomalies exceeding 0.58°C, this event did not expand eastward and yielded neutral anomalies in the El Niño 1+2 region (Lyon & Barnston 2005). These imbalances may be due to atmospheric and oceanic precursors during the event's development; air disturbances, such as westerly winds, are among the primary precursors (Fedorov 2002). Similarly, Kelvin waves can be precursors to events in the Eastern and Central Pacific. When they propagate eastward, they deepen the thermocline and weaken the trade winds (Capotondi et al. 2015). In addition, through atmospheric and oceanic teleconnections, oscillation events can cause environmental variability in certain areas, such as the effect of SST anomalies from the Central and Eastern Pacific towards sea level pressure (SLP) in the North Pacific (Yu & Kim 2011).

The lack of synchronization across regions raises questions about whether a single region should be used to define an ENSO event in the Pacific basin (Lyon & Barnston 2005). One approach to mitigating bias by considering ENSO indices uniformly across the entire area is to understand regional variability in SST anomalies better (Gergis et al. 2006). The SST anomaly analysis of the main hydrographic features in the EPO showed differences with the indices included in this study. For example, the ONI, El Niño 3, and El Niño 4 regions' trends in 2000 were towards La Niña conditions. Still, quadrants with neutral conditions predominated, with negative anomalies observed only in the NECC and CRD. Likewise, the indices showed El Niño conditions between 2002 and 2003; nevertheless, the quadrant proportion with positive anomalies was below 40%, while the fraction with

neutral conditions was slightly above 60%; positive anomalies in 2002 were observed only in the NECC, SEC, and CRD time series. These results are consistent with those of Lagerloef et al. (2003), who used empirical orthogonal functions to investigate anomalies in surface currents and SST, revealing that trade wind displacement might have affected El Niño 2002/03. In our analysis, we observed that the positive SST anomalies were predominantly located in the Central Pacific rather than near the American coastline.

Another difference was observed when comparing the negative trends in all indices during 2016 and 2017 with the quadrant counts, which showed a very low percentage of negative values. The present analysis identified dominant positive anomalies during 2016, 2017, and 2018, in contrast with Feng et al. (2020), who documented part of the 2017/18 La Niña evolution in the Southeastern Pacific using wind stress and deep-water data. However, it is worth noting that the impacts of this event were less pronounced than those of La Niña 2010/11. Nonetheless, there were instances in which the indices and the current analysis aligned, such as during the weak La Niña 2010/11 and the El Niño 2014/15.

As previously mentioned, high correlations were observed between El Niño regions, despite reports indicating that the identification of ENSO events can lag by several months between the El Niño 3.4 and El Niño 4 regions (Trenberth & Stepaniak 2001). Similarly, high correlations with the sampled areas, particularly those closer to El Niño regions, could be attributed to the meridional and zonal transport mechanism of SST anomalies in the EPO current systems (Sprintall et al. 2020). Conversely, sampled areas with low correlations with El Niño regions were located farther away, in the northern (CC and NEC) and southern (PC) extremes of the EPO. In addition, the CC is fed by the North Pacific Current (~50°N) and flows latitudinally towards the equator (Huyer et al. 1998, Checkley & Barth 2009), subsequently feeding into the NEC (Fiedler & Lavín 2017). For the PC, the lack of alignment with Pacific basin-wide ENSO indices is likely due to the high environmental variability within this current, suggesting the influence of localized events such as the coastal El Niño (Ramírez & Briones 2017, Takahashi & Martínez 2019).

Among the indices considered in this study, ONI is one of the most widely used to identify ENSO events and to explain the impacts of anomalous SST on marine species. For instance, Farchadi et al. (2019) assessed ENSO impacts on the spatial distribution of billfish, focusing on a strong La Niña (2000) and a weak El Niño (2003). However, in the present analysis, La Niña 2000 was not prominent in ERSST quadrant counts, while El Niño 2002/03 was only slightly detected in the NECC, SEC, and CRD. Neither event showed uniformity across all EPO areas. Likewise, Feng et al. (2022) used the ONI to identify ENSO events and determine variations in habitat suitability of jumbo squid (*Dosidicus gigas*) and jack mackerel (*Trachurus murphyi*). There were differences in ENSO event definitions compared to our study; according to those authors, 2007, 2009, 2014, and 2017 had neutral conditions in the southern EPO. In contrast, the results of the current study indicated negative anomalies in 2007 and positive ones in 2009. In 2014 and 2017, the curves represented positive anomalies, while the ONI classified these years as neutral. On the other hand, Possamai et al. (2018) analyzed temporal variability in estuarine fish composition in a Brazilian lagoon using ENSO events as indicators of local climate variability. The weak El Niño event of 2002/03, identified by the ONI, was used in their study; however, 2003 was predominantly neutral, as observed in this analysis. Moreover, while ENSO events are recognized for their teleconnections (Whetton & Rutherfurd 1994), the linkage between the ONI and the Atlantic Ocean remains less well-defined. Due to these inconsistencies, we consider that relying on a single index without accounting for local SST anomalies may introduce bias when explaining changes in species presence.

The SST anomaly time series analysis showed a greater frequency of warm events than cold ones, with the former characterized by greater intensity and a larger spatial extent, especially after 2014. Burgers & Stephenson (1999) have noted that one factor contributing to the predominance of El Niño over La Niña in recent years is the high skewness in the SST distribution in the EPO. Similarly, Ramos-Rodriguez et al. (2012) analyzed regime shifts in SST anomalies and their association with solar irradiance and found a correlation between elevated atmospheric solar energy and the occurrence of positive SST anomalies during the 1950-2010 timeframe. The period from 2000 to 2010 was characterized by marked anomalies near zero or exhibiting positive trends, and by a notable absence of strong ENSO events. The former aligns with the findings of the present study, where the most robust ENSO event identified was El Niño 2014/16.

Limitations

Understanding the spatial extent of cool and warm anomalous events in the EPO is highly relevant, given their impacts on various components of the marine food

chain and the associated economic losses, which have been well documented. While this study describes these events, it is important to acknowledge its primary limitation: its exclusive reliance on sea surface temperature data, without considering the broader context of events in deeper layers of the water column. Therefore, future research characterizing ENSO events may include temperatures from subsurface layers more comprehensively, since it has been demonstrated that subsurface temperatures are highly effective for identifying these anomalous events (Yu et al. 2011). Similarly, for studies seeking to incorporate ENSO events as independent variables, it is strongly recommended to consider not only the regional extent of SST anomalies within the EPO but also their vertical variations. When possible, incorporating additional factors that influence the intensity of these events is advisable, including thermocline dynamics, solar irradiance, and wind patterns, among other relevant variables (Wang & Fiedler 2006, Ramos-Rodríguez et al. 2012, Peng et al. 2020).

CONCLUSIONS

This analysis has shown discrepancies between El Niño indices and the regional anomaly assessment. La Niña 2000/01 and El Niño 2002/03 were not detected in all the EPO. Conversely, the warming observed in several regions during 2017 was not identified by the indices. Therefore, it is recommended to conduct a region-specific analysis of sea surface temperature anomalies to evaluate the impacts of cool and warm events, rather than relying on an index that may not accurately capture localized conditions.

The California, North Equatorial, and Peru currents, located farther from the El Niño 3, El Niño 4, and El Niño 3.4 regions, showed the largest differences with the indices estimates (correlations between 0.177 and 0.576). In contrast, hydrographic features located closer to those regions (NECC and SEC) exhibited conditions more aligned with the indices, showing higher correlations (0.783-0.949).

Finally, over the last 20 years, warm events were more frequent and spatially more extensive than cold ones, with a dominance of quadrants with positive anomalies (>500 quadrants) during seven years, while only four years showed relevant negative anomalies (190 to 250 quadrants).

Author contribution

A. Buenfil-Ávila: conceptualization, validation, methodology, formal analysis, writing-original draft; S. Ortega-García: conceptualization, validation, methodology, formal analysis, writing-original draft, project administration, and supervision; U. Jakes-Cota: review and editing; R. Moncayo-Estrada: review and editing; G. Reygondeau: review and editing; H. Villalobos: conceptualization, validation, methodology, formal analysis, writing-original draft, project administration, and supervision. All authors have read and accepted the final version of the manuscript.

Conflict of interest

The authors declare no conflict of interest.

ACKNOWLEDGMENTS

We thank the two anonymous reviewers for their suggestions and comments, which helped to improve this manuscript. ABA acknowledges financial support from SECIHTI (Secretaría de Ciencia, Humanidades, Tecnología e Innovación) and BEIFI-IPN (Beca de Estímulo Institucional de Formación de Investigadores del Instituto Politécnico Nacional). This study was supported by the Secretaría de Investigación y Posgrado del Instituto Politécnico Nacional through different projects: SIP20230385; SIP20240148; SIP20251226.

REFERENCES

An, S.I. & Wang, B. 2000. Interdecadal change of the structure of the ENSO mode and its impact on the ENSO frequency. Journal of Climate, 13: 2044-2055. doi: 10.1175/1520-0442(2000)013<2044:ICOTSO>2.0.CO;2

Ashok, K., Behera, S.K., Rao, S.A., et al. 2007. El Niño Modoki and its possible teleconnection. Journal of Geophysical Research: Oceans, 112: C11. doi: 10.1029/2006JC003798

Bakun, A. 1990. Global climate change and intensification of coastal ocean upwelling. Science, 247: 198-201. doi: 10.1126/science.247.4939.198

Belkin, I.M. 2009. Rapid warming of large marine ecosystems. Progress in Oceanography, 81: 207-213. doi: 10.1016/j.pocean.2009.04.011

Burgers, G. & Stephenson, D.B. 1999. The “normality” of El Niño. Geophysical Research Letters, 26: 1027-1030. doi: 10.1029/1999GL900161

Capotondi, A., Wittenberg, A.T., Newman, M., et al. 2015. Understanding ENSO diversity. Bulletin of the American Meteorological Society, 96: 921-938. doi: 10.1175/BAMS-D-13-00117.1

Checkley Jr., D.M. & Barth, J.A. 2009. Patterns and processes in the California Current System. Progress in Oceanography, 83: 49-64. doi: 10.1016/j.pocean.2009.07.028

Chen, X., Qiu, B., Du, Y., et al. 2016. Interannual and interdecadal variability of the North Equatorial Countercurrent in the western Pacific. Journal of Geophysical Research: Oceans, 121: 7743-7758. doi: 10.1002/2016JC012190

Di Lorenzo, E. & Mantua, N. 2016. Multi-year persistence of the 2014/15 North Pacific marine heatwave. Nature Climate Change, 6: 1042-1047. doi: 10.1038/nclimate3082

Díaz-Delgado, E., Crespo-Neto, O. & Martínez-Rincón, R.O. 2021. Environmental preferences of sharks bycaught by the tuna purse-seine fishery in the eastern Pacific Ocean. Fisheries Research, 243: 106076. doi: 10.1016/j.fishres.2021.106076

Farchadi, N., Hinton, M.G., Thompson, A.R., et al. 2019. Modeling the dynamic habitats of mobile pelagic predators (*Makaira nigricans* and *Istiompax indica*) in the eastern Pacific Ocean. Marine Ecology Progress Series, 622: 157-176. doi: 10.3354/meps12996

Fedorov, A.V., 2002. The response of the coupled tropical ocean-atmosphere to westerly wind bursts. Quarterly Journal of the Royal Meteorological Society: A Journal of the Atmospheric Sciences, Applied Meteorology and Physical Oceanography, 128: 1-23. doi: 10.1002/qj.200212857901

Fedorov, A.V. & Philander, S.G. 2000. Is El Niño changing? Science, 288: 1997-2002. doi: 10.1126/science.288.5473.199

Félix-Salazar, L.A., Marín-Enríquez, E., Aragón-Noriega, E.A., et al. 2024. Analysis of the swordfish *Xiphias gladius* Linnaeus, 1758 catches by the pelagic longline fleets in the eastern Pacific Ocean. Journal of Marine Science and Engineering, 12: 496. doi: 10.3390/jmse12030496

Feng, Z., Yu, W. & Chen, X. 2022. Concurrent habitat fluctuations of two economically important marine species in the southeast Pacific Ocean off Chile in relation to ENSO perturbations. Fisheries Oceanography, 31: 123-134. doi: 10.1111/fog.12566

Feng, L., Zhang, R.H., Yu, B., et al. 2020. Roles of wind stress and subsurface cold water in the second-year cooling of the 2017/18 La Niña event. Advances in Atmospheric Sciences, 37: 847-860. doi: 10.1007/s00376-020-0028-4

Fiedler, P.C. & Lavín, F. 2017. Oceanographic conditions of the eastern tropical Pacific. In: Glynn, P., Manzello, D.P. & Enochs, I.C. (Eds.). Coral reefs of the eastern tropical Pacific: Persistence and loss in a dynamic environment. Springer, Berlin, pp. 59-84.

Fiedler, P.C. & Talley, L.D. 2006. Hydrography of the eastern tropical Pacific: A review. Progress in Oceanography, 69: 143-180. doi: 10.1016/j.pocean.2006.03.008

Gergis, J., Braganza, K., Fowler, A., et al. 2006. Reconstructing El Niño-Southern Oscillation (ENSO) from high-resolution palaeoarchives. Journal of Quaternary Science: Published for the Quaternary Research Association, 21: 707-722. doi: 10.1002/jqs.1070

Gibble, C., Duerr, R., Bodenstein, B., et al. 2018. Investigation of a large-scale common murre (*Uria aalge*) mortality event in California, USA, in 2015. Journal of Wildlife Diseases, 54: 569-574. doi: 10.7589/2017-07-179

Hanley, D.E., Bourassa, M.A., O'Brien, J.J., et al. 2003. A quantitative evaluation of ENSO indices. Journal of Climate, 16: 1249-1258. doi: 10.1175/1520-0442(2003)16<1249:AQEOEI> 2.0.CO;2

Horii, T. & Hanawa, K. 2004. A relationship between the timing of El Niño onset and subsequent evolution. Geophysical Research Letters, 31: 019239. doi: 10.1029/2003GL019239

Hu, D., Wu, L., Cai, W., et al. 2015. Pacific western boundary currents and their roles in climate. Nature, 522: 299-308. doi: 10.1038/nature14504

Huang, B., Thorne, P.W., Banzon, V.F., et al. 2017. Extended reconstructed sea surface temperature, version 5 (ERSSTv5): upgrades, validations, and intercomparisons. Journal of Climate, 30: 8179-8205. doi: 10.1175/JCLI-D-16-0836.1

Huyer, A., Barth, J.A., Kosro, P.M., et al. 1998. Upper-ocean water mass characteristics of the California Current, summer 1993. Deep Sea Research Part II: Topical Studies in Oceanography, 45: 1411-1442. doi: 10.1016/S0967-0645(98)80002-7

Kessler, W.S. 2006. The circulation of the eastern tropical Pacific: A review. Progress in Oceanography, 69: 181-217. doi: 10.1016/j.pocean.2006.03.009

Kug, J.S. & Ham, Y.G., 2011. Are there two types of La Niña? Geophysical Research Letters, 38: 048237. doi: 10.1029/2011GL048237

Lagerloef, G.S., Lukas, R., Bonjean, F., et al. 2003. El Niño Tropical Pacific Ocean surface current and temperature evolution in 2002 and outlook for early 2003. Geophysical Research Letters, 30: 017096. doi: 10.1029/2003GL017096

Legendre, P. & Legendre, L. 1998. Numerical ecology (Vol. 20). Developments in environmental modelling. Elsevier, Amsterdam.

Lehodey, P., Bertrand, A., Hobday, A.J., et al. 2021. ENSO impact on marine fisheries and ecosystems. In: McPhaden, M.J., Santoso, A. & Cai, W. (Eds.). El Niño Southern Oscillation in a changing climate. American Geophysical Union, Washington D.C., pp. 429-451.

Lellouche, J.M., Le Galloudec, O., Drévillon, M., et al. 2013. Evaluation of global monitoring and forecasting systems at Mercator Ocean. Ocean Science, 9: 57-81. doi: 10.5194/os-9-57-2013

Lengaigne, M. & Vecchi, G.A. 2010. Contrasting the termination of moderate and extreme El Niño events in coupled general circulation models. Climate Dynamics, 35: 299-313. doi: 10.1007/s00382-009-0562-3

Lyon, B. & Barnston, A.G. 2005. The evolution of the weak El Niño of 2004-2005. US CLIVAR Variations, 3: 1-4.

McCabe, R.M., Hickey, B.M., Kudela, R.M., et al. 2016. An unprecedented coastwide toxic algal bloom linked to anomalous ocean conditions. Geophysical Research Letters, 43: 10-366. doi: 10.1002/2016GL070023

National Marine Fisheries Service (NMFS). 2017. Fisheries economics of the United States, 2015. Government Printing Office. NOAA Technical Memorandum, NMFS-F/SPO-170: 247.

Peng, Q., Xie, S.P., Wang, D., et al. 2020. Eastern Pacific wind effect on the evolution of El Niño: Implications for ENSO diversity. Journal of Climate, 33: 3197-3212. doi: 10.1175/JCLI-D-19-0435.1

Possamai, B., Vieira, J.P., Grimm, A.M., et al. 2018. Temporal variability (1997-2015) of trophic fish guilds and their relationships with El Niño events in a subtropical estuary. Estuarine, Coastal and Shelf Science, 202: 145-154. doi: 10.1016/j.ecss.2017.12.019

R Core Team. 2023. R: a language and environment for statistical computing. R Foundation for Statistical Computing. [http://www.R-project.org]. Reviewed: November 20, 2023.

Ramírez, I.J. & Briones, F. 2017. Understanding the El Niño costero of 2017: The definition problem and challenges of climate forecasting and disaster responses. International Journal of Disaster Risk Science, 8: 489-492. doi: 10.1007/s13753-017-0151-8

Ramos-Rodríguez, A., González-Rodríguez, E., Villalobos, H., et al. 2020. Historical SST warming events in the northeastern Pacific: How unique is the Warm Blob? Revista de Biología Marina y Oceanografía, 55: 110-118. doi: 10.22370/rbmo.2020.55.2.2496

Ramos-Rodríguez, A., Lluch-Cota, D.B., Lluch-Cota, S.E., et al. 2012. Sea surface temperature anomalies, seasonal cycle, and trend regimes in the eastern Pacific coast. Ocean Science, 8: 81-90. doi: 10.5194/os-8-81-2012

Sprintall, S., Cravatte, B., DeWitt, Y., et al. 2020. Chapter 15: ENSO Oceanic teleconnections. In: McPhaden, M., Santoso, A. & Cai, W. (Eds.). El Niño Southern Oscillation in a changing climate. American Geophysical Union, Washington D.C., pp. 337-360.

Svetunkov, I. 2017. Statistical models underlying functions of 'smooth' package for R. Working Paper of Department of Management Science, Lancaster University, 1: 1-52.

Svetunkov, I. 2023. smooth: Forecasting Using State Space Models. R package version 4.0.0, [https://CRAN.R-project.org/package=smooth]. Reviewed: February 20, 2025.

Svetunkov, I. & Petropoulos, F. 2017. Old dog, new tricks: a modelling view of simple moving averages. International Journal of Production Research, 56: 6034-6047. doi: 10.1080/00207543.2017.1380326.

Takahashi, K. & Martínez, A.G. 2019. The very strong coastal El Niño in 1925 in the far-eastern Pacific. Climate Dynamics, 52: 7389-7415. doi: 10.1007/s00382-017-3702-1

Tan, S. & Zhou, H. 2018. The observed impacts of the two types of El Niño on the North Equatorial Countercurrent in the Pacific Ocean. Geophysical Research Letters, 45: 079273. doi: 10.1029/ 2018 GL079273

Timmermann, A., An, S.I., Kug, J.S., et al. 2018. El Niño-southern oscillation complexity. Nature, 559: 535-545. doi: 10.1038/s41586-018-0252-6

Trenberth, K.E. & Hoar, T.J. 1996. The 1990-1995 El Niño-Southern Oscillation event: Longest on record. Geophysical Research Letters, 23: 57-60. doi: 10.1029/95GL03602

Trenberth, K.E. & Stepaniak, D.P. 2001. Indices of El Niño evolution. Journal of Climate, 14: 1697-1701. doi: 10.1175/1520-0442(2001)014<1697:LIOENO>2.0.CO;2

Villalobos, H. & González-Rodríguez, E. 2022. Satin: Visualisation and analysis of ocean data derived from satellites. [https://github.com/hvillalo/satin]. Reviewed: November 10, 2023.

Wang, C. & Fiedler, P.C. 2006. ENSO variability and the eastern tropical Pacific: A review. Progress in

Oceanography, 69: 239-266. doi: 10.1016/j.pocean.2006.03.004

Whetton, P. & Rutherfurd, I. 1994. Historical ENSO teleconnections in the Eastern Hemisphere. Climatic Change, 28: 221-253. doi: 10.1007/BF01104135

Whitney, F.A. 2015. Anomalous winter winds decrease 2014 transition zone productivity in the NE Pacific. Geophysical Research Letters, 42: 428-431. doi: 10.1002/2014GL062634

Received: November 14, 2024; Accepted: October 12, 2025

Yu, J.Y. & Kim, S.T. 2011. Relationships between extratropical sea level pressure variations and the central Pacific and eastern Pacific types of ENSO. Journal of Climate, 24: 708-720. doi: 10.1175/2010JCLI3688.1

Yu, J.Y., Kao, H.Y., Lee, T., et al. 2011. Subsurface ocean temperature indices for Central-Pacific and Eastern-Pacific types of El Niño and La Niña events. Theoretical and Applied Climatology, 103: 337-344. doi: 10.1007/s00704-010-0307-6